

## Research Article

# Uniform versus Nonuniform Scaling of Normal Modes Predicted by *Ab Initio* Calculations: A Test on 2-(2,6-Dichlorophenyl)-N-(1,3-thiazol-2yl) Acetamide

Amrish K. Srivastava,<sup>1</sup> Anoop K. Pandey,<sup>2</sup> Saurabh Pandey,<sup>1</sup> Prakash S. Nayak,<sup>3</sup> B. Narayana,<sup>3</sup> B. K. Sarojini,<sup>3</sup> and Neeraj Misra<sup>1</sup>

<sup>1</sup> Department of Physics, University of Lucknow, Lucknow, Uttar Pradesh 226007, India

<sup>2</sup> Department of Physics, Govt. D. P. G. College, Dantewada, Chhattisgarh 494449, India

<sup>3</sup> Department of Studies in Chemistry, Mangalore University, Mangalagangothri, Karnataka 574199, India

Correspondence should be addressed to Neeraj Misra; [neerajmisra1@gmail.com](mailto:neerajmisra1@gmail.com)

Received 22 February 2014; Revised 14 May 2014; Accepted 14 May 2014; Published 10 July 2014

Academic Editor: Rolf W. Berg

Copyright © 2014 Amrish K. Srivastava et al. This is an open access article distributed under the Creative Commons Attribution License, which permits unrestricted use, distribution, and reproduction in any medium, provided the original work is properly cited.

A test on calculated vibrational modes of 2-(2,6-dichlorophenyl)-N-(1,3-thiazol-2yl) acetamide using *ab initio* density functional method has been performed. The calculated harmonic vibrational frequencies are scaled via two schemes, uniform,  $\nu_{\text{scaled}} = 0.9648\nu_{\text{calculated}}$ , and nonuniform,  $\nu_{\text{scaled}} = 22.1 + 0.9543\nu_{\text{calculated}}$ . Scaled vibrational modes are compared with experimental FTIR bands. A good correlation is shown between scaled frequencies with the correlation coefficient,  $R^2 = 0.99638-0.99639$ . This clearly shows that both schemes efficiently reproduce observed spectrum. However, a close investigation of individual normal modes reveals that nonuniform scaling performs much better than uniform scaling especially in the high frequency region.

## 1. Introduction

*Ab initio* quantum chemical methods are reliable tools for extracting valuable information about any chemical system. Currently available *ab initio* methods are capable of reproducing experimental IR spectra of rigid and small- as well as medium-size molecules. In many chemical systems, the theoretically calculated frequencies and intensities of vibrational modes closely resemble the experimentally observed values. Hence, it may be expected that the normal modes analysis from theoretically predicted force field reflects well the modes of vibrations in a real molecule. Normal-mode analysis is commonly employed in the interpretation of the vibrational spectra of molecules [1–4]. However, there are some limitations of the model used to calculate the vibrational frequencies. These limitations include the effect of electron correlation [5] and basis set deficiencies as well as inter- and intramolecular interactions. It needs to be emphasized that the calculated frequencies represent vibrational signature of the molecule in its gas (isolated) phase, unlike experimental

spectra which are recorded in liquid or solid phase of sample with impurity. This is experimentally verified that  $\nu_{\text{gas}} > \nu_{\text{liquid}} > \nu_{\text{solid}}$  [6]. On comparing the vibrational spectra, it is observed that, at places where calculated frequencies come out to be lower than the experimental frequencies, weak intermolecular interactions may be taking place. From a practical point of view, the main disadvantage of vibrational spectroscopy is the lack of a direct spectra-structure relation. *Ab initio* calculations follow the approximation that the chemical bonds are elastic, but it is not the case especially at higher range of frequencies due to anharmonicity of vibrations [7]. Thus, the computed frequencies within this Born-Oppenheimer approximation [8] need to be properly scaled. These anharmonic vibrations mainly include torsions and inversions, such as the umbrella modes of halomethyl radicals [9]. Similarly, in lower range of frequencies (where nearly all modes are rotational), the interaction of modes of vibration as well as molecular interaction takes place very strongly which certainly affect the calculated frequencies.

The motivation for predicting or simulating vibrational spectra is to make vibrational spectroscopy a more practical tool [10–12]. In this respect, it is not only desirable but also essential to have calculated frequencies very close to their observed values. This can usually be expected by appropriate scaling of calculated frequencies. Appropriate scaling method is still a fundamental problem existing in the literature, even today. Merrick et al. had calculated some scale factors using harmonic approximation but these factors did not work well in the region where mixing of several bands occurred [13]. Later on, Alecu et al. have calculated new scale factors within harmonic approximation for a number of theoretical methods [14]. They tested a lot of functional systems, for example, electronic model chemistries, single-level wave, doubly hybrid density, neglect-of-diatomic-differential-overlap, and so forth. On the other hand, Mauricio Alcolea Palafox derived some scaling equations by statistical correlation and suggested that these scaling equations give more satisfactory result as compared to constant scale factors [15–17].

In present paper, we perform a critical survey on the scaling of vibrational frequencies of 2-(2,6-dichlorophenyl)-N-(1,3-thiazol-2-yl) acetamide by using two different schemes. The first scheme is based on a constant scale factor as suggested by Alecu et al. which we call “uniform scaling.” The second scheme is based on a scaling equation as recommended by Palafox et al., which we refer to as “nonuniform scaling.”

## 2. Computational Methods

Our *ab initio* calculations employ a hybrid form of density functional, B3LYP in conjunction with 6–31+G(d,p) basis set for geometry optimization of the test molecule. The B3LYP combines Becke’s three-parameter exchange term [18] with the functional devised by Lee-Yang-Parr to treat electron correlation [19]. Vibrational frequency calculations are performed using optimized geometry at the same level of theory. The calculated frequencies are scaled by two different schemes as below.

For uniform scaling [13],

$$\nu_{\text{scaled}} = 0.9648\nu_{\text{calculated}} \quad (1)$$

For nonuniform scaling [15],

$$\nu_{\text{scaled}} = 22.1 + 0.9543\nu_{\text{calculated}} \quad (2)$$

Gaussian 09 package [20] is used to perform all computations and assignments of calculated vibrational modes are made with the help of visual animation generated by GaussView 5.0 program [21].

## 3. Results and Discussion

First, we discuss some salient features of test molecule in condensed as well as isolated (gas) phase. The single crystal of 2-(2,6-dichlorophenyl)-N-(1,3-thiazol-2-yl) acetamide is grown by slow evaporation method (melting point = 489–491 K) [22]. A photograph of this crystal along with X-ray

spectrum can be found in supplementary information (see Figures S1 and S2 in Supplementary Material available online at <http://dx.doi.org/10.1155/2014/649268>). In crystal phase, molecules are linked by pairs of N–H···N hydrogen bonds as shown in Figure 1.

The measured X-ray crystallographic parameters are used to model an initial structure of isolated molecule for the process of geometry optimization. After optimization, we find a sofa shaped structure in which the mean plane of dichlorophenyl ring is almost perpendicular to that of thiazole ring as shown in Figure 2.

In Figure 3, we have shown a linear correlation between calculated and observed bond-lengths. Note that C–H bond-lengths are not included here. We find a good correlation with correlation coefficient ( $R^2$ ) of 0.9991 which suggests that our computational scheme is fully capable of reproducing the experimental geometry.

FTIR spectrum of test molecule is recorded by using Shimadzu-Model Prestige 21 spectrometer in the region 400–4000  $\text{cm}^{-1}$  with the sample (purity of 98%) in KBr pellet. The vibrational analysis of isolated molecule (Figure 2) is performed at the same level of theory as mentioned earlier. In Figure 4, we plot calculated IR and observed FTIR spectra for wavenumber region of 1800  $\text{cm}^{-1}$ –600  $\text{cm}^{-1}$ . The calculated wavenumbers are scaled by using (1) and (2). The assignments of all vibrational modes have been made along with their directions of polarization. Table 1 lists calculated and scaled wavenumbers of all vibrational modes as well as their assignments. For the sake of comparison, FTIR values of the most prominent modes are also included.

In Figures 5 and 6, we have shown the correlation between experimentally observed wavenumbers and theoretically scaled wavenumbers. We find the correlation coefficient of 0.99638–0.99639 which ensures that both scaling schemes are equivalently appropriate, at least in the present case. In order to compare these two scaling schemes for particular vibration mode, we divide our vibrational analysis into two categories.

**3.1. Higher Frequency Region (above 1400  $\text{cm}^{-1}$ ).** This region covers C–H stretching vibrations of phenyl ring and methylene group along with N–H as well as C=O stretching modes of amide group. N–H stretching mode is observed experimentally at 3203  $\text{cm}^{-1}$  and corresponding scaled frequencies are calculated at 3475  $\text{cm}^{-1}$  and 3459  $\text{cm}^{-1}$  by uniform scaling and nonuniform scaling, respectively. The apparent discrepancy between experimental and theoretical frequencies is a consequence of intermolecular hydrogen bonding present in condensed phase (see Figure 1) but absent in case of isolated molecule. The most prominent C–H mode associated with phenyl ring vibrations is seen at 3045  $\text{cm}^{-1}$  in FTIR which is scaled at 3090  $\text{cm}^{-1}$  and 3078  $\text{cm}^{-1}$  by our theoretical schemes.

The C=O stretching observed at 1687  $\text{cm}^{-1}$  is scaled at 1684 and 1688  $\text{cm}^{-1}$ , respectively. Similarly, C–C stretching of phenyl ring at 1550  $\text{cm}^{-1}$  corresponds to scaled values of 1546  $\text{cm}^{-1}$  and 1551  $\text{cm}^{-1}$ . The C–H stretching associated with

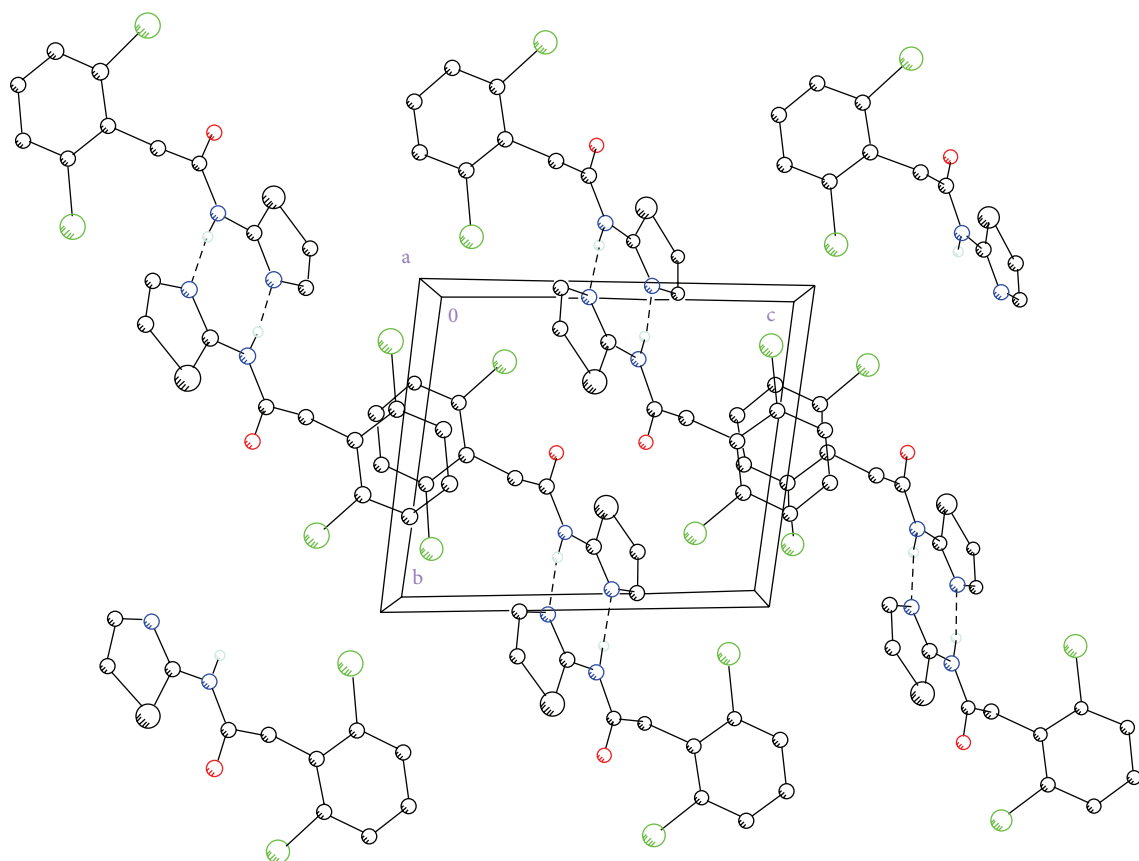


FIGURE 1: Crystal geometry of 2-(2,6-dichlorophenyl)-N-(1,3-thiazol-2-yl) acetamide. Intermolecular interactions are shown by broken lines.

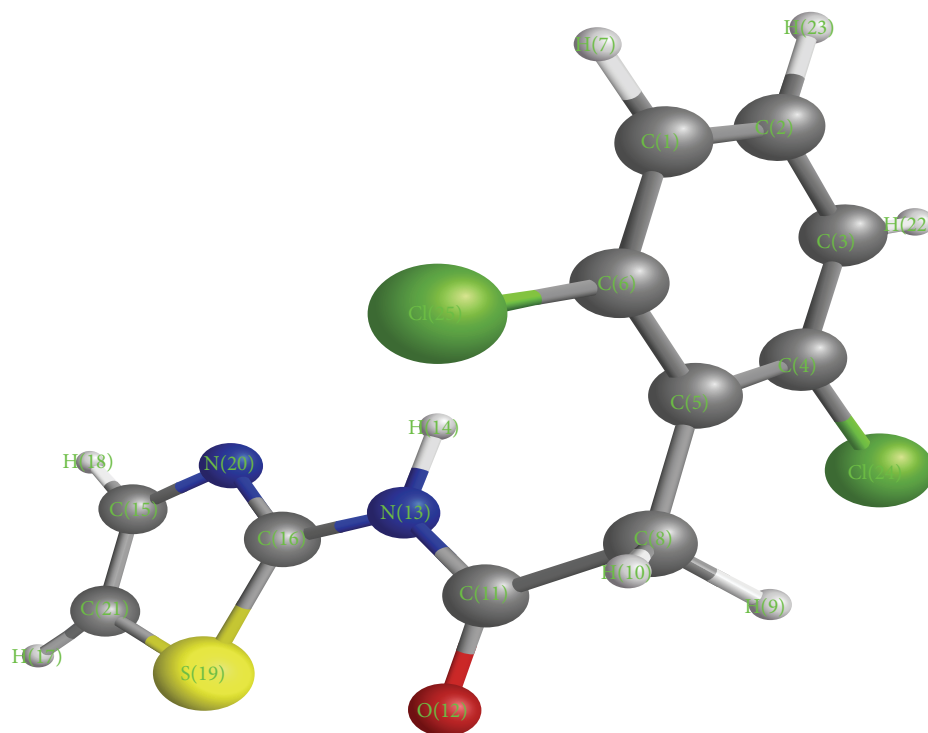


FIGURE 2: Molecular geometry of 2-(2,6-dichlorophenyl)-N-(1,3-thiazol-2-yl) acetamide optimized at B3LYP/6-31+G(d,p) level.

TABLE 1: Normal modes assignments and scaled frequencies for 2-(2,6-dichlorophenyl)-N-(1,3-thiazol-2-yl) acetamide. For comparison, observed FTIR bands are also given.

Calculated freq. $\text{cm}^{-1}$	Scaled freq. (1) $\text{cm}^{-1}$	Scaled freq. (2) $\text{cm}^{-1}$	FTIR freq. $\text{cm}^{-1}$	IR intensity a.u.	Assignment of vibrational modes	Direction of polarization
3602	3475	3459	3203	68	$\nu(13\text{N}-14\text{H})$	Along 13N-14H
3272	3156	3144		1	$\nu_s(15\text{C}-18\text{H}) + \nu_s(17\text{C}-21\text{H})$	Along 13H-11C
3233	3119	3107		8.78	$\nu_{as}(15\text{C}-18\text{H}) + \nu_s(17\text{C}-21\text{H})$	Per R1
3228	3114	3102		1.69	$\nu_{as}(3\text{C}-2\text{H}) + \nu(2\text{C}-23\text{H}) + \nu(1\text{C}-7\text{H})$	Along 6C-5H
3224	3110	3098		0.23	$\nu(3\text{C}-2\text{H}) + \nu(1\text{C}-7\text{H})$	Per R1
3203	3090	3078	3045	3.32	$\nu(3\text{C}-2\text{H}) + \nu(2\text{C}-23\text{H}) + \nu(1\text{C}-7\text{H})$	Along 2C-23H
3137	3026	3015		0.09	$\nu_{as}(9\text{H}-8\text{C}-10\text{H})$	Per R1
3093	2984	2973		3.43	$\nu(9\text{H}-8\text{C}-10\text{H})$	Along 11C-12O
1746	1684	1688	1687	266.85	$\nu(11\text{C}=12\text{O})$	Along 13N-14H
1627	1569	1574		9.20	$\nu(\text{C}-\text{C})\text{R2}$	Along R2
1603	1546	1551	1550	37.68	$\nu(\text{C}-\text{C})\text{R2}$	Per R1
1582	1526	1531		430.27	$\nu(\text{C}-\text{C})\text{R2} + \nu(\text{C}-\text{N})\text{R2} + \nu(6\text{C}-13\text{C}) + \beta(15-18\text{H})$	Per R2
1525	1471	1477		107.34	$\beta(15\text{C}-21\text{H}) + \beta(15\text{C}-18\text{H}) + \beta(13\text{N}-14\text{H})$	Along 11H-12O
1474	1422	1428	1436	9.00	Scissoring (9H-8C-10H) + $\beta(13\text{N}-14\text{H})$	Along 11H-12O
1468	1416	1423		63.64	$\beta(\text{C}-\text{H})\text{R2}$	Along R2
1465	1413	1420		16.52	$\beta(1\text{C}-7\text{H}) + \beta(3\text{C}-22\text{H}) + \beta(13\text{N}-14\text{H}) + \nu(5\text{C}-8\text{C})$	Per 14H plane
1459	1407	1414		26.22	Scissoring (9H-8C-10H) + $\beta(13\text{N}-14\text{H})$	Containing 13N-14H
1349	1301	1309		62.92	$\beta(21\text{C}-7\text{H}) + \beta(15\text{C}-18\text{H})$	Along 13N-16C
1335	1288	1296		4.25	Rocking (9H-8C-10H) + $\beta(\text{C}-\text{H})\text{R1}$	Along 8C-5C
1334	1287	1295	1286	1.05	$\tau(9\text{H}-8\text{C}-10\text{H}) + \beta(\text{C}-\text{H})\text{R1}$	Per R1
1306	1260	1268		112.91	$\beta(13\text{N}-14\text{H}) + \nu(16\text{C}-19\text{S})$	Plane containing 17N directed along R1
1251	1206	1215		1.41	$\beta(\text{C}-\text{N})\text{R2} + \tau(9\text{H}-8\text{C}-10\text{H})$	Per R1
1226	1182	1192		53.76	$\beta(1\text{C}-7\text{H}) + \beta(3\text{C}-22\text{H}) + \beta(15\text{C}-18\text{H}) + \text{rocking}(9\text{H}-8\text{C}-10\text{H})$	Along 8C-11C
1220	1177	1186		43.98	$\beta(15\text{C}-8\text{H}) + \beta(13\text{N}-14\text{H}) + \beta(3\text{C}-22\text{H}) + \text{rocking}(9\text{H}-8\text{C}-10\text{H})$	Along 17N-16C
1196	1153	1163		9.49	$\beta(\text{C}-\text{H})\text{R2} + \tau(9\text{H}-8\text{C}-10\text{H})$	Per R1
1181	1139	1149		30.16	$\beta(15\text{C}-18\text{H}) + \beta(13\text{N}-14\text{H})$	Along 13N-14H
1172	1130	1140	1141	16.73	$\tau(9\text{H}-8\text{C}-10\text{H}) + \beta(2\text{C}-23\text{H})$	Per R1
1101	1062	1072		13.16	$\beta(\text{C}-\text{H})\text{R2}$	Along 11C-12O
1088	1049	1060		9.84	Scissoring (18H-15C-21C-17H)	Along R2
1086	1047	1058		8.96	$\beta(3\text{C}-22\text{H}) + \beta(1\text{C}-7\text{H}) + \text{rocking}(9\text{H}-8\text{C}-10\text{H}) + \nu(6\text{C}-25\text{Cl})$	Along R1
987	952	963		0.33	$\gamma(\text{C}-\text{H})\text{R2}$	Plane containing 13N directed to R1
975	940	952	931	7.78	$\omega(9\text{H}-8\text{C}-10\text{H}) + \beta(\text{C}-\text{H})\text{R1}$	
939	905	918		41.74	Rocking (9H-8C-10H)	Per R1
909	877	889		0.06	$\gamma(1\text{C}-7\text{H}) + \gamma(3\text{C}-22\text{H})$	Along R2

TABLE I: Continued.

Calculated freq. $\text{cm}^{-1}$	Scaled freq. (1) $\text{cm}^{-1}$	Scaled freq. (2) $\text{cm}^{-1}$	FTIR freq. $\text{cm}^{-1}$	IR intensity a.u.	Assignment of vibrational modes	Direction of polarization
897	865	878		3.26	$\tau(18\text{H}-25\text{C}-21\text{C}-17\text{H})$	Per R1
882	850	863	856	6.68	In plane R1 bending	Along R1
855	824	838		3.10	Ring R2 breathing (9H-8C-10H)	Along R2
787	759	773	785	38.64	$\gamma(\text{C}-\text{H})\text{R}3$	In between 13N-14H
783	755	769	761	23.20	$\gamma(\text{C}-\text{H})\text{R}2 + \text{R}1$ breathing	Plane containing 13N directed to R1
767	740	754		67.40	In plane R2 bending + $\tau(9\text{H}-8\text{C}-10\text{H})$	Per R1
718	692	707	692	39.09	$\gamma(15\text{C}-18\text{H}) + \gamma(21\text{C}-17\text{H})$	Per R1
661	637	652		11.08	$\beta(\text{R}1) + \text{R}(9\text{H}-8\text{C}-10\text{H})$	Along 16C-21H
631	608	624		29.47	$\gamma(13\text{N}-14\text{H}) + \gamma(16\text{C}-20\text{N}-15\text{C})$	Per R1
624	602	617	592	8.67	$\gamma(\text{C}-\text{H})\text{R}1 + \gamma(19\text{S}-15\text{C}-20\text{C}) + \text{Rocking}(9\text{H}-8\text{C}-10\text{H})$	Per R1
563	543	559		2.16	$\gamma(\text{R}1) + \gamma(13\text{N}-14\text{H}) + \text{rocking}(9\text{H}-8\text{C}-10\text{H})$	Per R1
559	539	555		12.84	Twisting R1 + rocking (9H-8C-10H)	Per R2
511	493	509		11.14	$\gamma(\text{R}1) + \gamma(13\text{N}-14\text{H})$	Per R1
486	468	485		8.55	$\gamma(1\text{C}-2\text{C}-3\text{C}) + \gamma(\text{CH})\text{R}2 + \omega(9\text{H}-8\text{C}-10\text{H})$	Per R2
478	461	478		4.74	$\beta(\text{R}2) + \text{R}(9\text{H}-8\text{C}-10\text{H})$	Per R2
424	409	426		4.28	$\gamma(4\text{C}-24\text{Cl}) + \tau(1\text{C}-2\text{C}-3\text{C})$	Along 10C-11O
404	389	407		5.09	$\beta(\text{CH})\text{R}2 + \text{R}(9\text{H}-8\text{C}-10\text{H}) + \beta(\text{C}-\text{Cl})\text{R}2$	Per R1

Note.  $\nu$ : stretching;  $\nu_s$ : symmetric stretching;  $\nu_{as}$ : asymmetric stretching;  $\beta$ : in-plane-bending;  $\gamma$ : out-of-plane bending;  $\omega$ : wagging;  $\tau$ : torsion.

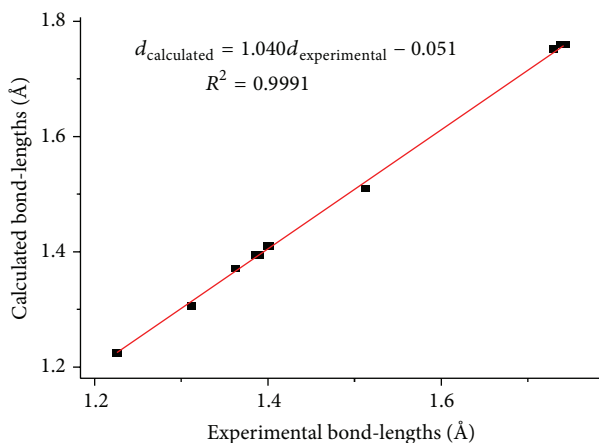


FIGURE 3: Correlation between calculated and experimental bond-lengths of 2-(2,6-dichlorophenyl)-N-(1,3-thiazol-2-yl) acetamide.

methylene group is found to be coupled with N-H stretching mode at  $1436 \text{ cm}^{-1}$  which is theoretically scaled at  $1422 \text{ cm}^{-1}$  and  $1428 \text{ cm}^{-1}$  by uniform scaling and nonuniform scaling schemes, respectively.

3.2. Lower Frequency Region (below  $1400 \text{ cm}^{-1}$ ). In this region, the bending modes associated with ring systems and

various groups are generally observed. The in-plane bending of methylene group observed at  $1286 \text{ cm}^{-1}$  and  $1141 \text{ cm}^{-1}$  is coupled with phenyl ring vibration. The uniform scaling gives these modes at  $1287 \text{ cm}^{-1}$  and  $1130 \text{ cm}^{-1}$  while nonuniform scaling calculates at  $1295 \text{ cm}^{-1}$  and  $1140 \text{ cm}^{-1}$ , respectively. Similarly, out of plane bending of methylene coupled with phenyl ring at  $931 \text{ cm}^{-1}$  in FTIR is scaled at  $940 \text{ cm}^{-1}$  and  $952 \text{ cm}^{-1}$  by our theoretical schemes.

The in-plane bending of thiazole ring is observed at  $856 \text{ cm}^{-1}$  against scaled values of  $850 \text{ cm}^{-1}$  and  $863 \text{ cm}^{-1}$ . On the other hand, the bending of phenyl ring observed at  $785 \text{ cm}^{-1}$  is scaled at  $759 \text{ cm}^{-1}$  and  $773 \text{ cm}^{-1}$ . Furthermore, the coupling of vibrations of both rings is observed at  $761 \text{ cm}^{-1}$  corresponding to scaled values of  $755 \text{ cm}^{-1}$  and  $769 \text{ cm}^{-1}$ . Moreover, even lower normal modes at  $692 \text{ cm}^{-1}$  and  $592 \text{ cm}^{-1}$  associated with bending of thiazole rings are scaled at  $692 \text{ cm}^{-1}$  and  $602 \text{ cm}^{-1}$  by uniform scaling method, whereas at  $707 \text{ cm}^{-1}$  and  $617 \text{ cm}^{-1}$  by nonuniform scaling scheme.

The above discussion suggests that scaled wavenumbers by both schemes successfully explain observed bands in case of title molecule, giving a good correlation with experimental frequencies (see Figures 5 and 6). The comparative response of two scaling schemes is given in terms of wavenumber difference between observed and scaled bands plotted in Figure 7. A close investigation on Figure 7 reveals that

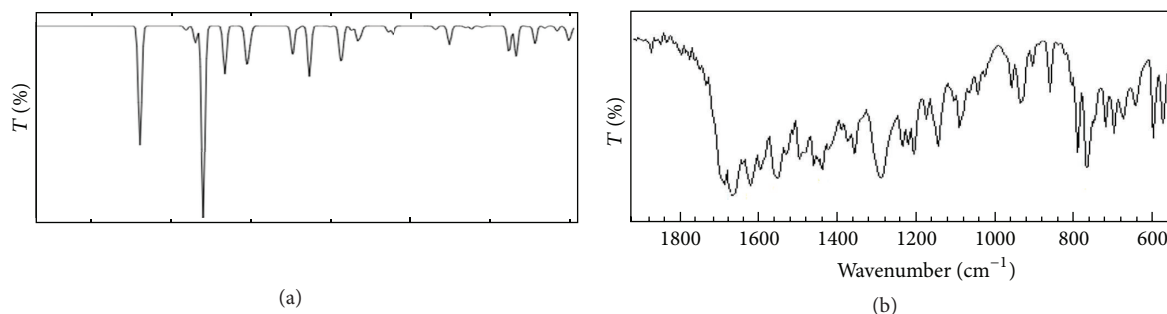


FIGURE 4: Calculated (a) and experimental (b) vibrational IR spectra of 2-(2,6-dichlorophenyl)-N-(1,3-thiazol-2-yl) acetamide in the region 1800–600  $\text{cm}^{-1}$ .

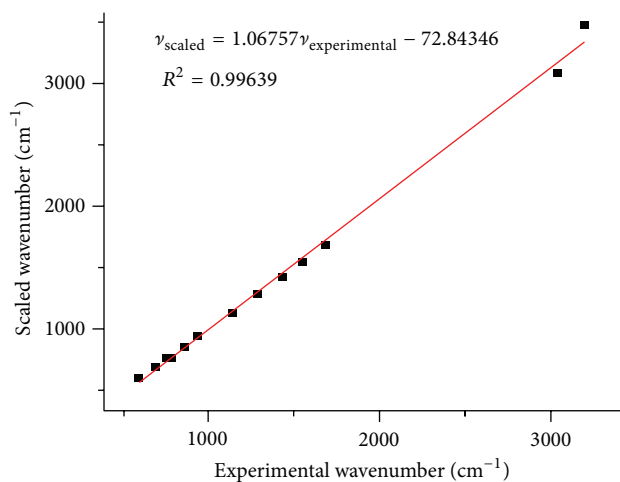


FIGURE 5: Correlation between calculated (scaled) and experimental wavenumbers of 2-(2,6-dichlorophenyl)-N-(1,3-thiazol-2-yl) acetamide. Scaling is performed by a scale factor (equation (1)).

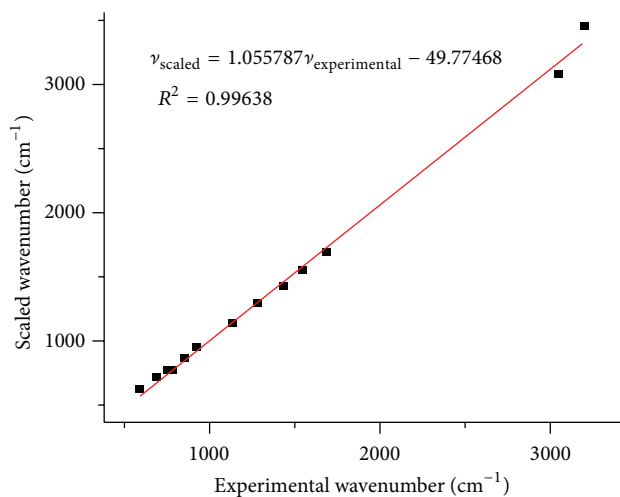


FIGURE 6: Correlation between calculated (scaled) and experimental wavenumbers of 2-(2,6-dichlorophenyl)-N-(1,3-thiazol-2-yl) acetamide. Scaling is performed by a scaling equation (equation (2)).

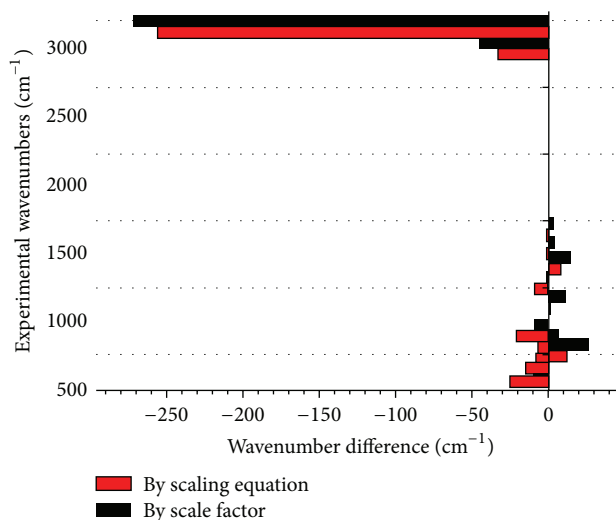


FIGURE 7: The difference between scaled and experimental wavenumbers for 2-(2,6-dichlorophenyl)-N-(1,3-thiazol-2-yl) acetamide.

nonuniform scaling performs much better than uniform scaling especially in the high frequency region. Thus, the calculated vibrational modes should be scaled by appropriate scaling equation to account for anharmonicity in vibrations. For lower frequency region, where discrepancies between calculated and observed wavenumbers are observed mainly due to mixing of vibrational modes and the effect of electron correlation, both scaling schemes perform equally well.

#### 4. Conclusions

We have performed a test on the scaling of calculated vibrational bands in case of 2-(2,6-dichlorophenyl)-N-(1,3-thiazol-2-yl) acetamide, adopting two different scaling schemes, namely, scale factor and scaling equation. Scaled normal modes are compared with observed vibrational bands. The validity of both schemes is established by the correlation between theoretically scaled frequencies and experimentally observed frequencies with the coefficient of 0.9964. The analysis of individual modes has revealed that both schemes perform equally well for the lower range of frequencies below 1400  $\text{cm}^{-1}$  (torsion, wagging, etc.). In case

of high frequency region (above  $1400\text{ cm}^{-1}$ ) where most of the stretching modes occur, scaling equation provides more accurate vibrational bands as compared to scale factor. To be specific, C–H stretching of phenyl ring observed at  $3045\text{ cm}^{-1}$  (in present case) is better represented by  $3078\text{ cm}^{-1}$  (by scaling equation) rather than by  $3090\text{ cm}^{-1}$  (by scale factor) at B3LYP/6-31+G(d,p) theory. Thus, the present assessment is supposed not only to assist further studies on the prediction or simulation of vibrational spectra of new molecules but also to assign more accurate vibrational modes for previously reported molecules in the literature.

## Conflict of Interests

The authors declare that there is no conflict of interests regarding the publication of this paper.

## Acknowledgment

Ambrish K. Srivastava wishes to thank Council of Scientific and Industrial Research (CSIR), New Delhi, India, for providing a research fellowship.

## References

- [1] N. Misra, O. Prasad, L. Sinha, and A. Pandey, "Molecular structure and vibrational spectra of 2-formyl benzonitrile by density functional theory and ab initio Hartree-Fock calculations," *Journal of Molecular Structure: THEOCHEM*, vol. 822, no. 1-3, pp. 45-47, 2007.
- [2] S. A. Siddiqui, A. Dwivedi, N. Misra, and N. Sundaraganesan, "Computational note on vibrational spectra of Tyramine hydrochloride: DFT study," *Journal of Molecular Structure*, vol. 847, no. 1-3, pp. 101-102, 2007.
- [3] A. K. Srivastava, B. Narayana, B. K. Sarojini, and N. Misra, "Vibrational, structural and hydrogen bonding analysis of *N*'-[(*E*)-4-Hydroxybenzylidene]-2-(naphthalen-2-yloxy) acetohydrazide-combined density functional and atoms-in-molecule based theoretical studies," *Indian Journal of Physics*, vol. 88, pp. 547-556, 2014.
- [4] A. K. Srivastava, A. K. Pandey, B. Narayana, B. K. Sarojini, P. S. Nayak, and N. Misra, "Normal modes, molecular orbitals and thermochemical analyses of 2, 4 and 3, 4 dichloro substituted phenyl-*N*-(1, 3-thiazol-2-yl) acetamides: DFT study and FTIR spectra," *Journal of Theoretical Chemistry*, vol. 2014, Article ID 125841, 10 pages, 2014.
- [5] J. A. Pople, H. B. Schlegel, R. Krishnan et al., "Molecular orbital studies of vibrational frequencies," *International Journal of Quantum Chemistry*, vol. 15, pp. 269-278, 1981.
- [6] M. Silverstein, G. C. Basseler, and C. Morill, *Spectrometric Identification of Organic Compounds*, Wiley, New York, NY, USA, 1981.
- [7] J. A. Pople, A. P. Scott, M. W. Wong, and L. Radom, "Scaling factors for obtaining fundamental vibrational frequencies and zero-point energies from HF/6-31G\* and MP2/6-31G\* harmonic frequencies," *Israel Journal of Chemistry*, vol. 33, pp. 345-350, 1993.
- [8] [http://en.wikipedia.org/wiki/Born-Oppenheimer\\_approximation](http://en.wikipedia.org/wiki/Born-Oppenheimer_approximation).
- [9] P. Marshall, G. N. Srinivas, and M. Schwartz, "A computational study of the thermochemistry of bromine- and iodine-containing methanes and methyl radicals," *The Journal of Physical Chemistry A*, vol. 109, no. 28, pp. 6371-6379, 2005.
- [10] S. A. Siddiqui, A. Dwivedi, P. K. Singh et al., "Molecular structure, vibrational spectra and potential energy distribution of protopine using ab initio and density functional theory," *Journal of Structural Chemistry*, vol. 50, no. 3, pp. 411-420, 2009.
- [11] A. K. Pandey, S. A. Siddiqui, A. Dwivedi, K. Raj, and N. Misra, "Density functional theory study on the molecular structure of loganin," *Spectroscopy*, vol. 25, no. 6, pp. 287-302, 2011.
- [12] S. A. Siddiqui, A. Dwivedi, A. Pandey et al., "Molecular structure, vibrational spectra and potential energy distribution of colchicine using ab initio and density functional theory," *Journal of Computer Chemistry, Japan*, vol. 8, no. 2, pp. 59-72, 2009.
- [13] I. M. Alecu, J. Zheng, Y. Zhao, and D. G. Truhlar, "Computational thermochemistry: scale factor databases and scale factors for vibrational frequencies obtained from electronic model chemistries," *Journal of Chemical Theory and Computation*, vol. 6, no. 9, pp. 2872-2887, 2010.
- [14] J. P. Merrick, D. Moran, and L. Radom, "An evaluation of harmonic vibrational frequency scale factors," *The Journal of Physical Chemistry A*, vol. 111, no. 45, pp. 11683-11700, 2007.
- [15] M. Alcolea Palafox, "Scaling factors for the prediction of vibrational spectra. I. Benzene molecule," *International Journal of Quantum Chemistry*, vol. 77, no. 3, pp. 661-684, 2000.
- [16] M. Alcolea Palafox and V. K. Rastogi, "Quantum chemical predictions of the vibrational spectra of polyatomic molecules. The uracil molecule and two derivatives," *Spectrochimica Acta A: Molecular and Biomolecular Spectroscopy*, vol. 58, no. 3, pp. 411-440, 2002.
- [17] M. Alcolea Palafox, J. L. Núñez, and M. Gil, "Accurate scaling of the vibrational spectra of aniline and several derivatives," *Journal of Molecular Structure*, vol. 593, pp. 101-131, 2002.
- [18] A. D. Becke, "Density-functional thermochemistry. III. The role of exact exchange," *The Journal of Chemical Physics*, vol. 98, no. 7, pp. 5648-5652, 1993.
- [19] C. Lee, W. Yang, and R. G. Parr, "Development of the Colle-Salvetti correlation-energy formula into a functional of the electron density," *Physical Review B*, vol. 37, no. 2, pp. 785-789, 1988.
- [20] M. J. Frisch, G. W. Trucks, H. B. Schlegel et al., *Gaussian 09 Revision B.01*, Gaussian, Wallington, Conn, USA, 2010.
- [21] R. Dennington, T. Keith, and J. Millam, *GaussView Ver. 5.01*, Semichem, Shawnee, Kan, USA, 2005.
- [22] P. S. Nayak, B. Narayana, H. S. Yathirajan, J. P. Jasinski, and R. J. Butcher, "2-(2,6-Dichlorophenyl)-*N*-(1,3-thiazol-2-yl)acetamide," *Acta Crystallographica Section E: Structure Reports Online*, vol. 69, no. 4, p. o523, 2013.



**Hindawi**

Submit your manuscripts at  
<http://www.hindawi.com>

